Risk assessment of an offshore wind turbine and remaining useful life (RUL) estimation of the power converter. Improving availability by prioritising failures with higher risk to operation.

Marco Sepulveda [(1)], Peter Davies [(2)], Mark Spring [(2)], Dr Jonathan Shek[(1)], Dr Philipp Thies[(1)], Dr Erkan Oterkus[(1)]
(1)Industrial Doctorate Centre for Offshore Renewable Energy (IDCORE) - (The University of Edinburgh, University of Strathclyde, University of Exeter)
(2) Lloyd's Register EMEA
*Lloyd's Register EMEA, 25 Union Terrace, Aberdeen, AB10 1NN, United Kingdom
Marco.Sepulveda@lr.org / s1152152@ed.ac.uk

EXECUTIVE SUMMARY

By 2014, almost 2500 offshore wind turbines were installed in Europe representing 8GW of capacity connected to the grid and, there is a growing market penetration for the next years. Offshore wind farm operators are facing many challenges related to disparate data sources utilisation for O&M logistic optimisation. Therefore, the decision-making process needs to be based on sound analysis of the wind farm information or data available.

According to several technical reports operation and maintenance (O&M) cost could reach until 30% of the levelised cost of energy (LCOE). Understanding the reliability of an offshore wind turbine and the resources required to maintain it is crucial to reduce O&M costs and thus, to reduce the levelised cost of energy (LCOE). There is a need to reduce unnecessary tasks, prioritise the most urgent tasks, improve usage of vessels, crew and technicians, reduce the cost of spare parts held and schedule preventative maintenance to minimise downtime and maximise revenue.

Currently, risk assessment plays an important role in the operation and maintenance (O&M) strategies of offshore wind farms. A comprehensive failure mode and effect analysis (FMEA) has been carried out to determine critical assemblies of a generic offshore wind turbine with an induction generator, three stages gearbox and monopile foundation. The main objectives of undertaking this comprehensive FMEA was to identify those failures with significant impact on the wind turbine operation and to identify or highlight areas of risk for maintainability and availability. The FMEA is validated with; widely-used data available in the public domain; Lloyd's Register's experience of working with wind farm operators and; Lloyd's Register experience of working on reliability of the mechanical system of different industrial sectors for decades. The FMEA is further augmented and updated by the use of on-going measurements from operating wind farms.

Yaw system, pitch system, power converter and gearbox have been identified in the FMEA as the most critical assemblies regarding risk to the turbine operation. Power converter analysis shows high failure rates and a large proportion of undetectable failures, therefore maintenance resources have been spent on fault finding with its corresponding cost. New approaches are necessary to tackle electrical or electronic failures, especially on the power converter. To improve overall reliability, a method to estimate the remaining useful life (RUL) of a fully-rated converter in a variable speed wind turbine is proposed using data commonly available for offshore wind farm operators. Studies show that the economic impact is dominated by failures related to power electronic components such as IGBTs and capacitors due to their higher repair cost. Mathematical models have been developed to correlate turbine operation variables and environmental conditions with failure root causes to define wear and maintenance actions based on the probability of failure.

INTRODUCTION

The power electronic converter has shown high failure rates. Failures of the power converter are becoming more unacceptable due to accessibility issues and a strong impact on the power grid. More precisely, power converter has been identified as one of the most important causes of failure of variable speed offshore wind turbines [1]. Reliability of power electronics is a critical and developing need for offshore wind farm operators; the assessment is essential for design as well as for the lifetime extension which leads to reduction of energy cost [2].

Damage accumulation or aging of power converter modules is mainly due to different properties of adjacent materials, especially different coefficients of thermal expansion of adjacent layers, see Figure 1. Bond wire lift-off and solder delamination has been identified as the main failure modes [3]. Based on [4], the main source of stress that produce power electronic components failures is temperature cycling. Figure 2 shows that 55% of the failure mechanism are triggered by thermal activity, followed by vibration with 20%.

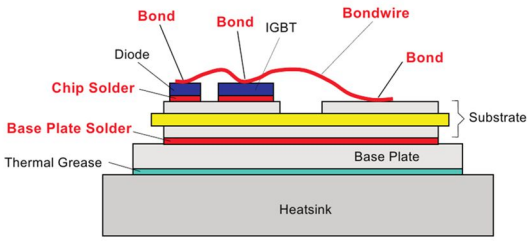

Figure 1. Power converter module structural details [3] [5].

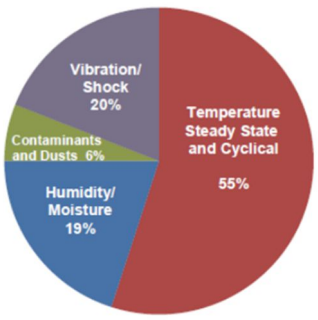

Figure 2. Source of stresses with impact on electronic components [4].

A systematic physics-based method has been proposed to predict the damage accumulation of power converter of offshore wind turbines as shown in Figure 3. This paper explains the approach undertaken to assess critical assemblies of offshore wind farms and each block of the flow diagram of condition estimation of power electronic components taking into account thermal cycling as the main source of stress.

RISK ASSESSMENT

The FMEA was performed for the functional modes of each system, subsystem, assembly and component following the British standard BS EN 60812:2006. The main objectives of undertaking this comprehensive FMEA are to identify those failures with significant impact on the wind turbine operation and to identify or highlight areas of risk for maintainability and availability. The procedure allocates numerical values from 1 to 5 to each risk associated with a failure, using Severity, Occurrence and Detection as categories. The values of the ranking rise when the risk increases. These are then combined into a Risk Priority Number (RPN), which can be used to analyse the system. By targeting high RPN values the most risky components and assemblies can be further studied. RPN is calculated by multiplying the Severity, Occurrence and Detection of the risk, as it is shown in Table 1.

The FMEA is conducted in accordance with the international standard IEC described in the British Standard BS EN 60812:2006 “Analysis techniques for system reliability - Procedure for failure mode and effects analysis (FMEA)”. This standard provides procedural steps necessary to perform the analyses identifying appropriate terms, assumptions, criticality measures and failure modes [6].

The analysis consists of the following five main stages:

- Establishment of the basic ground rules for the FMEA/FMECA and defining scope.

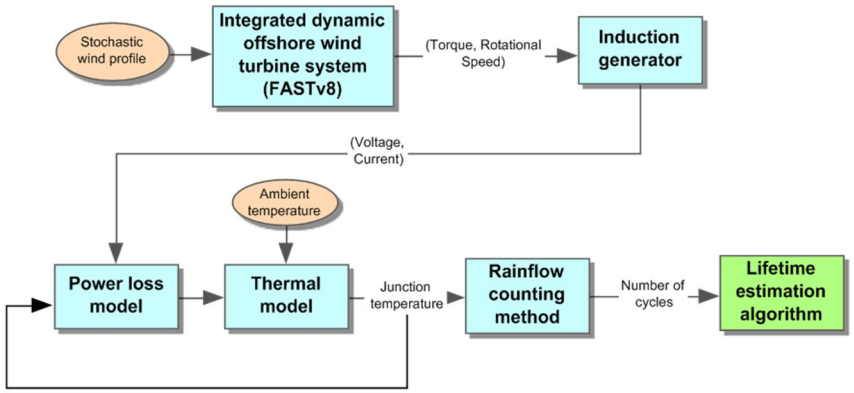

Figure 3. Remaining useful life estimation flow diagram.

- Defining systems structure including information on different system elements with their characteristics, performances, roles and functions.
- Executing the FMEA using the appropriate worksheet with a pre-defined system boundary and level of the analysis.
- Summarizing and reporting of the analysis to include any conclusions and recommendations made.
- Updating the FMEA as the new inputs are incorporated.

Table 1. Critical assemblies ranked by risk priority number.

Assembly	Risk Priority Number (RPN)
Frequency Converter	38.3
Pitch System	33.9
Yaw System	30.8
Gearbox	30.1
Nacelle Auxiliaries	29.0
Control & Comm. System	28.1
Generator	27.6
Main Shaft Set	27.0
Tower	26.0
Power Electrical System	25.0
Foundation	24.6
Cable	24.0
Blade	21.0
Hydraulics System	18.0
Auxiliary Electrical System	17.8
Transition Piece	17.3
Nacelle Structure	16.0
Hub	12.0

Table 1 shows that the four most critical assemblies are the power converter, pitch system, yaw system and gearbox. Power converter is considered a critical assembly mainly due to the unpredictability of electrical failures and impact of those failure on the turbine operation.

WIND PROFILE AND INTEGRATED DYNAMIC TURBINE SYSTEM

In order to assess the damage accumulation of the power converter assessed in the FMEA, it is necessary to realistically emulate the same operational conditions in terms of turbine structural and electro-mechanical behaviour, and wind profile.

To achieve realistic results, load cases proposed by the IEC 61400-3 (power production category) using the aero-hydro-servo-elastic simulator FASTv8 developed by National Renewable Energy Laboratory (NREL), is used. The standard proposes a number of design situations representing the various modes of operation that an offshore wind turbine would experience during its operation life; each design situation leads to a number of Design Load Cases (DLCs). The IEC standard distinguishes two types of load cases, ultimate and fatigue load cases and recommends appropriate load factors to be associated with these load cases to evaluate the structural integrity. The selected load cases are shown in

Table 2. The turbulent full wind field is created by TurbSim [7] and couple with FASTv8.

The analysis is based on the 3 bladed horizontal 3.6MW turbine model, variable speed control system, mounted on a monopile with a rigid foundation, induction generator, 3 stage gearbox and fully power converter. Wind condition are site specific.

GENERATION OF OPERATIONAL CONDITIONS FOR PREDICTION PURPOSES

To simulate random processes a Markov Chain Monte Carlo (MCMC) tool is selected assuming stationary transition probabilities. A sequence of random elements of some set, such as wind speeds or load cases, can be defined by MCMC if the conditional distribution X_{n+1} given $X_1,X_2\ldots,X_n$ depends on X_n only [9]. Figure 4 shows a transition graph and transition matrix which are an example of a discrete MCMC where each event in the sequence only depends only on the events occurring directly before. For instance, when the current state is load case 1 (LC1), there is a probability of 0.6 to move to LC2, then there is a probability of 0.3 to stay in LC2, a probability of 0.1 to go back to LC1, a probability of 0.4 to move to LC3 and so on. Therefore it is possible to generate future scenarios of wind profile and operational condition by applying MCMC with probabilities distribution of load cases and wind speeds (Figure 5).

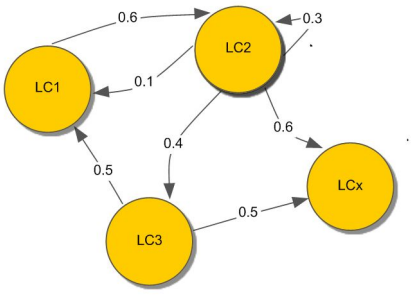

	LC1	LC2	LC3	LCx
LC1	0	0.6	0	0
LC2	0.1	0.3	0.4	0.6
LC3	0.5	0	0	0.5
LCx	0	0	0	0

Figure 4. Discrete example of MCMC, transition graph and matrix.

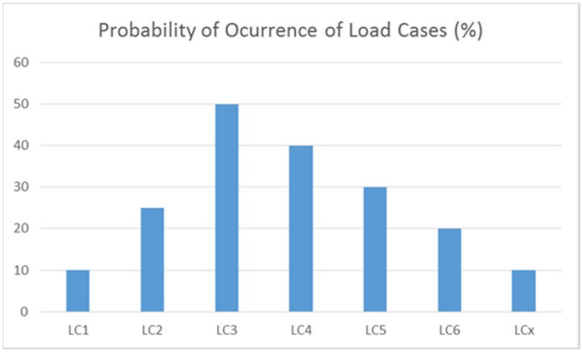

Figure 5. Example of probability distribution of load cases.

Table 2. Design load cases [8]

Design situation	DLC	Wind condition	Wind speed bins (with 2(m/s) increments)	Waves
Power production	1.2	NTM	3(m/s)<Vhub<25(m/S)	NSS joint probability distribution of Hs, Tp, Vhub
Power production plus occurrence of fault	2.4	NTM	3(m/s)<Vhub<25(m/S)	NSS, Hs = E[Hs|Vhub]
Start up	3.1	NWP	3(m/s)<Vhub<25(m/S)	NSS (or NWH), Hs = E[Hs|Vhub]
Normal shut down	4.1	NWP	3(m/s)<Vhub<25(m/S)	NSS (or NWH), Hs = E[Hs|Vhub]
Parked (standing still or idling)	6.4	NTM	Vin< 0.7Vref	NSS joint probability distribution of Hs, Tp, Vhub
Parked and fault conditions	7.2	NTM	Vin< 0.7V1	NSS joint probability distribution of Hs, Tp, Vhub
Transport, assembly, maintenance and repair	8.3	NTM	Vin< 0.7Vref	NSS joint probability distribution of Hs, Tp, Vhub

The simulation of each load case in FASTv8 gives the same outputs in the time domain which are related to structural loading, bending moments, and operation parameters such as rotational speed, wind speed and direction, shaft torques and power output.

Finally, the required inputs in the time domain, low speed shaft torque and rotational speed, for the remaining useful life estimation of the power converter are generated using MCMC. The ICE standard suggests simulation time for each load case, these time period are concatenated in order to generate the whole period in the future for prediction purposes. Figure 6 shows an example of a future scenario that an offshore wind turbine would experience during operation in the next 150 minutes.

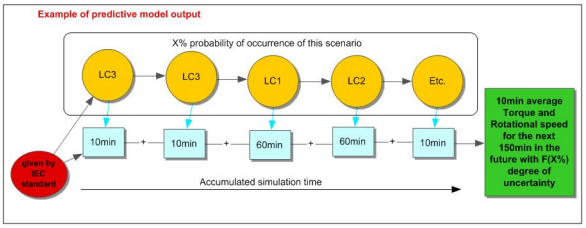

Figure 6. Example of future scenario generation.

INDUCTION GENERATOR MODEL

The details of the electrical drive to extract electrical variables are not usually modelled in FAST; instead, the focus is on getting the torque-speed curve correct, which effects turbine loads. For an induction machine, the most sophisticated built-in model available in FAST is the Thevenin-Equivalent Circuit (TEC) model. The analysed turbine uses a squirrel cage induction generator (SCIG) therefore a model to extract voltage and current variables is proposed to complement FAST simulations.

SCIG is a three-phase induction machine and has three windings in the stator and three windings more in the rotor, although, these can be imaginary. Generators can be described with the same set of equation than motors, see Figure 7. In order to simplify the equations is commonly used the following hypothesis [10]:

- Symmetric and balanced three-phase induction machine, with a single winding rotor (Squirrel cage simple) and constant gap.
- Material is assumed to be linear, that is to say, the iron saturation is discarded.
- The iron magnetic permeability is assumed to be infinite in front of the air permeability, which means that the magnetic flux density is radial to the gap.
- All kind of losses in the iron are neglected.
- Both the stator windings and the rotor windings represent distributed windings which always generate a sinusoidal magnetic field distribution in the gap

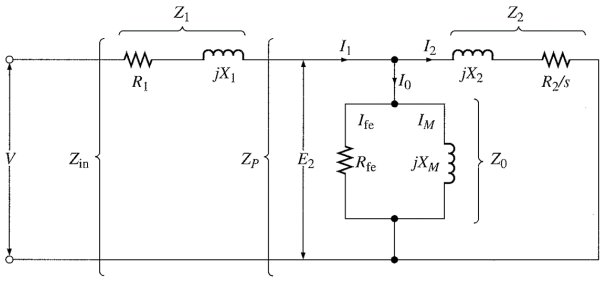

Figure 7. Induction machine simplified equivalent circuit

From the equivalent circuit is possible to derive the following equations:

$$s = \frac{n_s - n_r}{n_s}$$

$$Z_2 = \frac{R_2}{s} - jX_2$$

$$Z_P = \frac{Z_2 Z_0}{Z_2 + Z_0}$$

$$Z_{in} = Z_1 + Z_P$$

Where s is the slip which represent the difference between rotational speed and magnetic field rotation speed. R and X is electrical resistance and inductance, respectively.

The mechanical input power (Pm) and stator power output (Ps) are computed are based on the general relation between mechanical torque (Tm) and electrical power [11]:

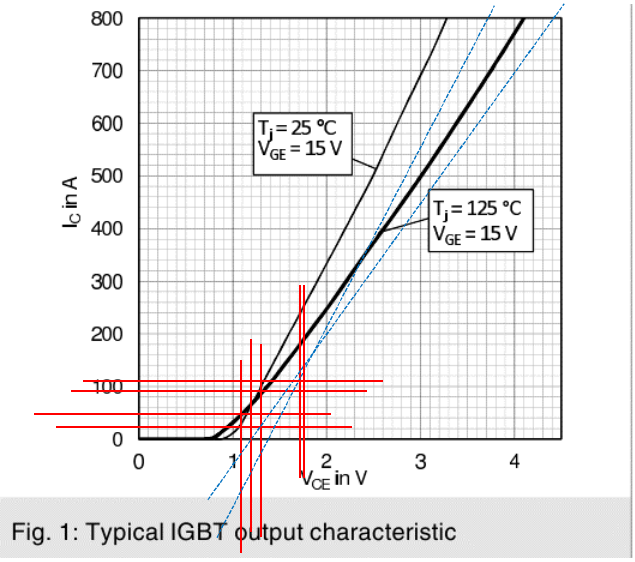

Fig. 1: Typical IGBT output characteristic

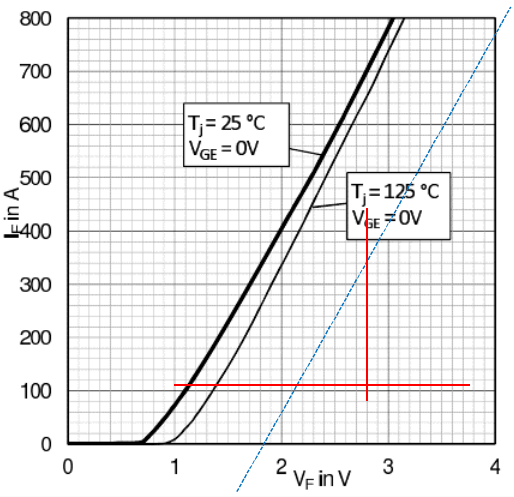

Fig. 2: Typical diode output characteristics

Figure 8. IGBT and Diode output characteristics [12].

$$P_m = T_m\omega_r;\ P_s = T_e\omega_s$$

Taking into account the SCIG efficiency (η)

$$P_s = \eta P_m$$

Therefore, AC voltage (V) and current (I) can be derived from the following relationships:

$$V = IZ_{in};\quad S = P_s + jQ$$

Where P is electrical active power and Q is reactive power.

POWER LOSSES OF INTEGRATED POWER MODULES

IGBT and Diode power losses can be divided into conduction losses (Pc), switching losses (Psw) and blocking (or leakage) losses (Pb) which is normally neglected.

$$Power\ losses = P_c + P_{sw} + P_b \approx P_c + P_{sw}$$

IGBT Conduction losses can be calculated as follow:

$$u_{CE}(i_c) = u_{CE0} + r_c i_c$$

Where u_{CE0} is the DC voltage source, r_C is the collector- emitter on-state resistance, i_c is the collector current. The same approach can be used for the anti-parallel diode:

$$u_D(i_D) = u_{D0} + r_D i_D$$

These parameters can be derived directly from the IGBT Datasheet (see Figure 8). In order to take into account ambient and junction temperature changes in every simulation step, the u_{CE0} and u_{D0} values are read from the diagram as temperature dependant.

Junction temperature values are extrapolated between 25°C and 125°C as follow:

For IGBT conduction losses calculation; rc-> Tj=25°C

Ic= a1*Vce + b1

For Vce=0.9V, Ic=0

For Vce=1.5V, Ic=160A

Therefore (a1,b1)=(266.67, -240)

Ic=266,67*Vce – 240 (Tj=25)

For IGBT conduction losses calculation, rc-> Tj=125°C

Ic= a2*Vce + b2

For Vce=0.8V, Ic=0

For Vce=3V, Ic=500A

Therefore (a2,b2)=(227.27 , -181,82)

Ic=227,27 *Vce – 181,82 (Tj=125)

To describe the temperature dependency of the curve for the conduction losses calculation

in the IGBTs the coefficients (a=rc,b) can be made temperature dependant [13]

$$rc(Tj)= a(Tj)=a_0+a_{01}*Tj$$

$$b(Tj)=b_0+b_{01}*Tj$$

Therefore, the relationship between collector current and voltage is given by:

$$Ic(Vce,Tj)=(a_0+a_{01}*Tj)*Vce + (b_0+b_{01}*Tj)$$

Where the parameters are:

$$(a_0+a_{01}*25)=a1 \text{ and } (a_0+a_{01}*125)=a2 \Rightarrow (a_0,a_{01})=(276.52, -0.394)$$

$$(b_0+b_{01}*25)=b1 \text{ and } (b_0+b_{01}*125)=b2 \Rightarrow (b_0,b_{01})=(-254.55, 0.582)$$

With r_c and r_D direved from Figure 8 and juction temperature dependant, the instantaneous value of the IGBT conduction losses can be estimated as follow:

$$p_{CT}(t) = u_{CE}(t) \cdot i_C(t) = u_{CE0} \cdot i_C(t) + r_C \cdot i_C^2(t)$$

If the average IGBT current value is Icav, and the rms value of IGBT current is I_{crms}, then the average losses can be expressed as:

$$P_{CT} = \frac{1}{T_{sw}} \int_0^{Tsw} p_T(t)dt = \frac{1}{T_{sw}} \int_0^{Tsw} (u_{CE0} \cdot i_C(t) + r_C \cdot i_C^2(t))dt$$

$$= u_{CE0} \cdot I_{cav} + r_C \cdot I_{crms}^2$$

The instantaneous value of the diode conduction losses is:

$$p_{CD}(t) = u_D(t) \cdot i_D(t) = u_{D0} \cdot i_F(t) + r_D \cdot i_D^2(t)$$

If the average diode current is I_{Dav}, and the rms diode current is I_{Drms}, the average diode conduction losses across the switching period (Tsw=1/fsw) are:

$$P_{CD} = \frac{1}{T_{sw}} \int_0^{Tsw} p_{CD}(t)dt = \frac{1}{T_{sw}} \int_0^{Tsw} (u_{D0} \cdot i_D(t) + r_D \cdot i_D^2(t))dt$$

$$= u_{D0} \cdot I_{Dav} + r_D \cdot I_{Drms}^2$$

Based on [14], the switching losses in the IGBT and the diode are the product of switching energies and the switching frequency (fsw). This characteristic is given by manufacturers as is shown in Figure 9.

$$P_{swM} = (E_{onM} + E_{offM}) \cdot f_{sw}$$

$$P_{swD} = (E_{onD} + E_{offD}) \cdot f_{sw} \approx E_{onD} \cdot f_{sw}$$

Finally, the total power losses in the IGBT and the diode can be expressed as the sum of the conduction and switching losses [5][14]:

$$P_T = P_{CT} + P_{swT} = u_{CE0} \cdot I_{cav} + r_C \cdot I_{crms}^2 + (E_{onT} + E_{offT}) \cdot f_{sw}$$

$$P_D = P_{CD} + P_{swD} = u_{D0} \cdot I_{Dav} + r_D \cdot I_{Drms}^2 + E_{onD} \cdot f_{sw}$$

As current values would be varying due to stochastic characteristic of the wind and turbulence intensity, the switching losses will be dependent on the input current using the slope in the curve [15]:

$$Eon+Eoff=e1*I \rightarrow e1=0.95$$

$$Err=e2*I \rightarrow e2=0.12$$

Pswm=0.95*I*fsw

Pswm=0.12*I*fsw

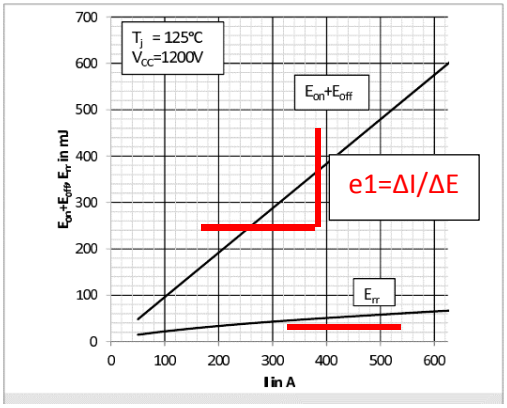

Figure 9. Typical energy losses [12]

THERMAL MODEL OF POWER CONVERTER

Power losses have to be conducted through the connection layers and insulation layers to the heat sink as it is shown in Figure 1. The heat dissipation generated during forward on-state and blocking state and during switching is expressed by the difference of temperatures

between the layers described by the following equation:

$$\Delta T_{j\text{-}s} = T_j - T_s$$

As it is mentioned before, different materials used during power converter module construction (Table 1) have different thermal expansion coefficient. This physics feature is represented by the thermal resistance and thermal impedance of the material which comprises geometry, conductivity and heat transfer area. The thermal resistance can be calculated as follow:

$$R_{th} = \frac{d}{\lambda \cdot A}$$

Where d is material thickness, ʎ is heat conductivity and A is heat flow area.

Table 3. Material commonly used on power converters [5].

Material	**Heat conductivity λ [W/(m*K)]**
Silicon	148
Copper	394
Aluminium	230
Silver	407
Molybdenum	145
Solders	~70
Al_2O_3-DBC	24
AlN DBC, AlN-AMB	180
AlSiC (75% SiC)	180

Similarly to an electrical circuit, the thermal model of the power converters can be expressed with an equivalent circuit as it is shown in Figure 10. Static thermal model (Rth) without base plate. Here power loss is the input (representing the current in an electrical circuit), the defence in temperature is the drop in the electrical voltage and thermal resistance represent the electrical resistance.

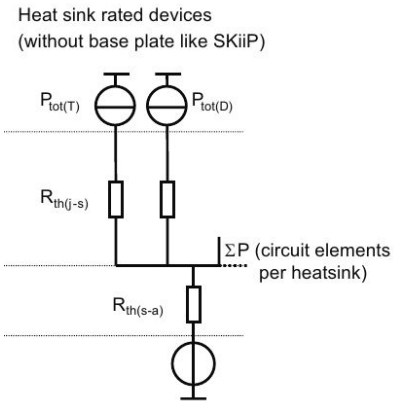

Figure 10. Static thermal model (Rth) without base plate.

The temperature differences ΔT over the thermal resistances are calculated for constant power dissipation P_T of the IGBT switches and Diodes inside the as follows:

$$\Delta T_{(j\text{-}s)} = T_j - T_s = P_T \cdot R_{th(j\text{-}s)} \text{/IGBT switch}$$

After losses have been calculated, temperature during stationary operation, can be calculated with the aid of thermal resistances Rth, final values of the Zth curve given by manufacturers (Figure 11).

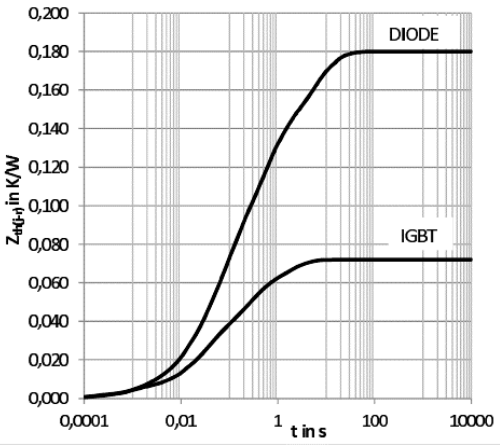

Figure 11. Transient thermal impedance [5,12]

Temperature calculation starts from the ambient temperature Ta outside to the inside as it is shown in the figure below.

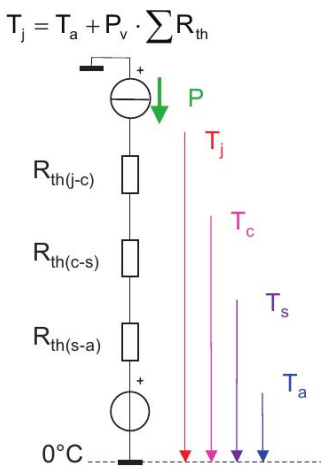

Figure 12. Temperature calculation process [5].

When there is more than one source of power loss on the heatsink, all the losses are added up. For example, for a power converter with 6 IGBTs and 6 Diodes, the total loss is used to calculate the heatsink temperature, as follows:

$$T_{heatsink} = n\left(P_{Total_{IBGTs}} + P_{Total_{Diodes}}\right) * R_{heatsink-ambient} + T_{ambient}$$

For example, if:

- $Rth(s\text{-}a)_{heatsink\text{-}ambient}$ = 0.1K/W
- n=6; number of components of a 3 phase rectifier/inverter, 6 IGBTs, 6 Diodes.

$$T_{heatsink}=Rth(s\text{-}a)_{heatsink\text{-}ambient}*(P_{IGBT\text{-}losses}+P_{D\text{-}losses})*N + Ta$$

$$Tj=Rth(j\text{-}s)_{IGBT}*P_{IGBT\text{-}losses} + T_{heatsink}$$

Likewise for Diode Tj calculation.

$$T_{heatsink}=Rth(s\text{-}a)_{heatsink\text{-}ambient}*(P_{IGBT\text{-}losses}+P_{D\text{-}losses})*N + Ta$$

$$Tj=Rth(j\text{-}s)_{Diode}*P_{D\text{-}losses} + T_{heatsink}$$

Now the junction temperature Tj for IGBTs and Diodes have been modified a new power loss has to be calculated as it is explain in Figure 13.

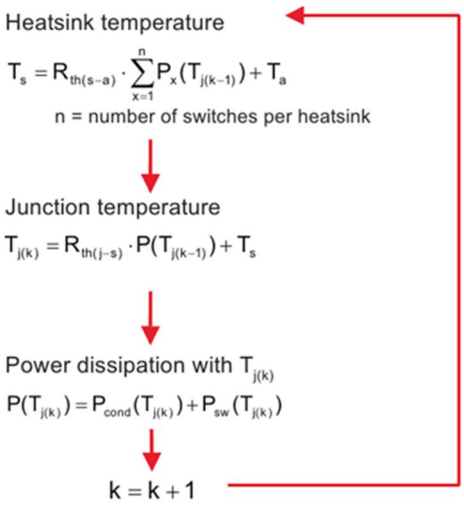

Figure 13. Process to calculate temperatures incorporating ambient temperature in each step [5]

Temperature fluctuations of internal connections of power modules produce ageing. As it is explained before, the fatigue of material is produced by thermal stress due to the different expansion coefficients of the connected materials or adjacent layers. During normal operation at frequencies of few Hz and especially at duty cycle operation, the internal connections of the layers in a power converter module will experience temperature cycling. At frequencies around 100Hz the temperature variation (ΔT) is small so low energy dissipation is counterbalanced by elastic deformation [5].

Rainflow counting method is applied to estimate the thermal cycles' frequency and amplitude ranges [4,16,17]. The rainflow counting method is adopted from material science to power electronics [17]. This method identifies in the data local highs and lows as peaks and valleys where the range between them are all considered to be half cycles. The algorithm pairs the half cycles to generate complete cycles regarding a mean. The term 'rainflow' comes from a part of the method where cycles are complete using arrows which look like water dripping from a roof (a peak), see Figure 14 [18].

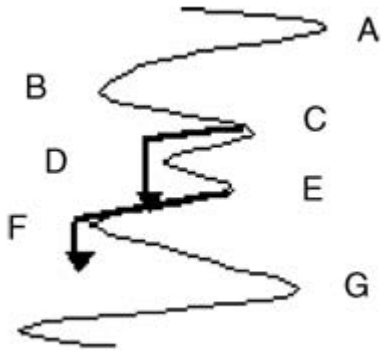

Figure 14. Rainflow cycles counting [18]

A script for the ASTM E 1049-85 (2005) Rainflow Counting Method is used using [19] as reference.

Based on [2][5], an empirical correlation between number of cycles to failure N_f and temperature cycling amplitude ΔT_j is given:

$$N_f = A \cdot \Delta T_j^{\alpha} \cdot e^{\left(\frac{E_a}{k_b \cdot T_{jm}}\right)}$$

Where:

- N_f represents the number of cycles to failure of the device.
- ΔT_j is the junction temperature thermal cycle amplitude.
- T_{jm} represents the mean absolute junction temperature.
- A, α and E_a are constant values given by the manufacturer.
- k_b represents Boltzman constant.

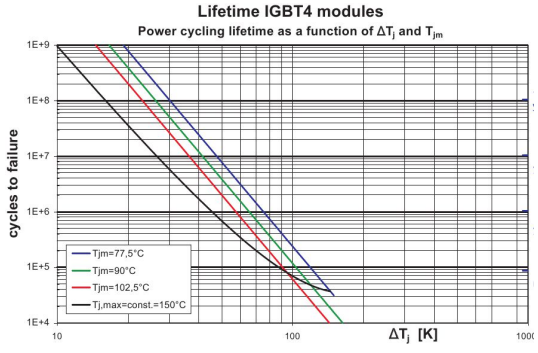

Figure 15. Dependency of the power cycling value n for IGBT4 modules as a function of the temperature cycling amplitude ΔT_j and the mean temperature T_{jm}

The proposed method to estimate the lifetime of power modules is based on Figure 15 which is provided by the manufacturer. Once temperature cycles are counted using the rainflow counting method, temperature cycling amplitude and the mean absolute junction temperature are calculated.

In Figure 15, an initial point is selected using the counted number of cycles and the calculated ΔT_j. then, the deference between final cycles to failure for the estimated mean junction temperature curve (blue, green, etc.) at the calculated ΔT_j and the initial point of counted number of cycles would result on the remaining cycles to failure.

IGBTs and Diodes junction temperature time series are separately analysed and then the lifetimes are combined using the Miner's rule [2].

A triangulation between counted numbers of thermal cycles associated with a period of prediction (in minutes or hours) and the remaining cycles to failure would result in a predicted failure date.

CONCLUSIONS

A comprehensive analysis and method are proposed to study the performance of power converters in offshore wind turbines from a reliability point of view. The FMEA has been a useful tool to analysis critical components in terms of risk to turbine operation and to identify components and their failure modes of fully rated power converters. The RPN allowed to recognise the need of controlling undetectable electrical failures in power converters impacting maintenance activities and therefore, impacting the cost of energy.

A physics-based method to estimate damage accumulation of IGBTs and Diodes and to predict the remaining useful life of power converters have been proposed. The simulations do not require a large computational effort, therefore it is suitable for day-to-day use.

REFERENCES

1. Ma K, Zhou D, Blaabjerg F. Evaluation and Design Tools for the Reliability of Wind Power Converter System. Journal of Power Electronics. 2015;15(5):1149–57.

2. Givaki K, Parker M, Jamieson P. Estimation of the power electronic converter lifetime in fully rated converter wind turbine for onshore and offshore wind farms. Power Electronics, Machines and Drives (PEMD 2014), 7th IET International Conference on. 2014. p. 1–6.

3. Degrenne N, Ewanchuk J, David E, Boldyrjew R, Mollov S. A Review of Prognostics and Health Management for Power Semiconductor Modules.

4. Wang H, Zhou D, Blaabjerg F. A reliability-oriented design method for power electronic converters. Applied Power Electronics Conference and Exposition (APEC), 2013 Twenty-Eighth Annual IEEE. 2013. p. 2921–8.

5. SEMIKRON. Application Manual Power Semiconductors. ISLE Verlag, a commercial unit ofthe ISLE Association; 2011.

6. Commission IE, others. Analysis Techniques for System Reliability: Procedure for Failure Mode and Effects Analysis (FMEA). International Electrotechnical Commission; 2006.

7. Jonkman BJ. TurbSim user's guide: Version 1.50. National Renewable Energy Laboratory Golden, Colorado; 2009;

8. Commission 2International Electrotechnical, others. Wind Turbines-Part 1: Design Requirements. 2007.

9. Geyer C. Introduction to Markov Chain Monte Carlo. Handbook of Markov Chain Monte Carlo. 2011;3–48.

10. Garcia JLD. Modeling and Control of Squirrel Cage Induction Generator with Full Power Converter Applied to Windmills. 2009.

11. Petersson A. Analysis, modeling and control of doubly-fed induction generators for wind turbines. Chalmers University of Technology; 2005.

12. semikron. SKIIP semikron datasheet. 2014.

13. Drofenik U, Kolar JW. A general scheme for calculating switching-and conduction-losses of power semiconductors in numerical circuit simulations of power electronic systems. Proceedings of the 2005 International Power Electronics Conference (IPEC'05), Niigata, Japan, April. 2005. p. 4–8.

14. Graovac D, Purschel M. IGBT power losses calculation using the data-sheet parameters-Application note. 2014-08-01] http://www infineon com. 2009;

15. Semikron. SkiiiP 513 semikron datasheet. 2014.

16. Lei T. Doubly-fed induction generator wind turbine modelling, control and reliability. The University of Manchester, Manchester, UK; 2014;

17. Ikonen M, others. Power cycling lifetime estimation of IGBT power modules based on chip temperature modeling. Acta Universitatis Lappeenrantaensis. Lappeenranta University of Technology; 2012;

18. Manwell JF, McGowan JG, Rogers AL. Wind energy explained: theory, design and application. John Wiley \& Sons; 2010.

19. Irvine T. Vibration data python: rainflow fatigue [Internet]. [cited 01-08/16]. Available from: https://vibrationdatapython.wordpress.com/?s=rainflow